Numerical Methods for Solving Time-Fractional Differential Equations

Dissertation submitted to
Visvesvaraya National Institute of Technology, Nagpur
in partial fulfillment of the requirements for the award of
the degree of

Master of Science
in
Mathematics

by

PRANSHU JAIN (MS23MTH011)

under the guidance of

Dr. PRADIP ROUL

Department of Mathematics
Visvesvaraya National Institute of Technology
Nagpur 440 010 (India)
Month Year (May 2025)

Numerical Methods for Solving Time-Fractional Differential Equations

Dissertation submitted to
Visvesvaraya National Institute of Technology, Nagpur
in partial fulfillment of the requirements for the award of
the degree of

Master of Science
in
Mathematics

by

PRANSHU JAIN (MS23MTH011)

under the guidance of

Dr. PRADIP ROUL

Department of Mathematics
Visvesvaraya National Institute of Technology
Nagpur 440 010 (India)

Month Year (May 2025)

©Visvesvaraya National Institute of Technology (VNIT) 2025

Department of Mathematics

Visvesvaraya National Institute of Technology, Nagpur

Declaration

I, PRANSHU JAIN, hereby declare that this dissertation titled **"Numerical Methods for Solving Time-Fractional Differential Equations"** is carried out by me in the Department of Mathematics of Visvesvaraya National Institute of Technology, Nagpur. The work is original and has not been submitted earlier whole or in part for the award of any degree/diploma at this or any other Institution / University.

PRANSHU JAIN

Date:

Certificate

This is to certify that the dissertation titled **"Numerical Methods for Solving Time-Fractional Differential Equations"** is submitted by **PRANSHU JAIN** in partial fulfillment of requirements for the award of the degree **Master of Science in Mathematics** VNIT Nagpur. The work is comprehensive, complete and fit for final evaluation.

Dr. PRADIP ROUL

Assistant Professor

Department of Mathematics

VNIT,Nagpur

Head,Department of Mathematics

VNIT,Nagpur

Date:

Visvesvaraya National Institute of Technology, Nagpur

Non - Plagiarism Certificate

This certifies that the M.Sc. dissertation, **"Numerical Methods for Solving Time-Fractional Differential Equations"**, authored by PRANSHU JAIN (Enrollment No. MS23MTH011, ID No. 30266), has undergone a thorough plagiarism check using TURNITIN software. The detected overlap falls within the permissible limits. A concise summary of the plagiarism report is provided below:

Signature:

Student Name: PRANSHU JAIN

Enrollment No: MS23MTH011

ID No: 30266

Dr. Pradip Roul

Assistant Professor

Department of Mathematics

VNIT, Nagpur

ACKNOWLEDGEMENT

It is with immense gratitude and deep respect that I acknowledge my supervisor, Dr. Pradip Roul, Assistant Professor in the Department of Mathematics at Visvesvaraya National Institute of Technology, Nagpur. His exceptional guidance and steadfast support were truly the bedrock of this project. I am profoundly thankful for his insightful mentorship, which extended far beyond academic counsel and enriched my understanding in numerous ways. This work would not have come to fruition without his active involvement.

I also wish to express my sincere appreciation to Dr. Pallavi Mahale, Professor and Head of the Department of Mathematics at VNIT, Nagpur, for her generous cooperation and the provision of outstanding resources throughout this endeavor. My sincere thanks extend to Dr. M. Devakar, Dr. Vijender Nallapu, my dedicated R.P.C. members. Their encouragement at each stage was invaluable. Furthermore, I am deeply grateful to all the faculty members of the Department of Mathematics at VNIT Nagpur for their consistent and unwavering support.

I am particularly thankful to Mr. Sameer Khandagale, Ph.D. research scholar, whose insightful guidance has been truly invaluable. His example has vividly demonstrated the vital role of dedication and commitment in realizing meaningful achievements. I also extend my sincere thanks to Mr. Vikas Kumar and Mr. Vivek Pathak, Ph.D. research scholars in the Department, for their generous gift of time, thoughtful suggestions, and engaging discussions throughout this entire process. To Miss Jyoti Yadav fellow Ph.D. research scholar, I offer my gratitude for their contributions in clarifying key concepts.

My heartfelt appreciation extends to my parents and cherished brother Dhruv, whose unwavering support, blessings, and encouragement have been a constant source of strength.Finally, I offer my deepest gratitude to the guiding force that has made the realization of this work possible.

PRANSHU JAIN

ABSTRACT

This project centers on the development of numerical methods for solving two distinct classes of time-fractional differential equations: the time-fractional Burgers' equation (TFBE) [1] and the time-fractional Fokker-Planck equation (TFFPE) [2].

Specifically:

- For the TFBE [1], a numerical scheme is constructed utilizing the L1 method [3] (with non-uniform mesh) for discretizing the temporal derivative and the standard finite difference method for spatial approximation.
- For the TFFPE [2], a numerical approach is formulated by coupling the L1 scheme [3] (with non-uniform mesh) for time discretization with a compact finite difference scheme for spatial discretization.

The stability of the proposed numerical schemes is established through the application of Von Neumann Fourier analysis, and the convergence properties of the method are rigorously investigated. The convergence analysis reveals that the numerical solutions for the model problems achieve an order of $O(h^2 + N^{-(2-\alpha)})$ for the TFBE [1] and $O(h^4 + N^{-(2-\alpha)})$ for the TFFPE [2], where h represents the spatial step size and N is the number of time steps.

List of Figures

5.1 3D graph of numerical solution of example 5.1.1 with $M = N = 64$. 39

5.2 3D graph of exact solution of example 5.1.1 with $M = N = 64$ 41

5.3 3D graph of error of example 5.1.1 41

5.4 3D graph of approximate solution of example 5.2.1 with $M = N = 50$ 43

5.5 3D graph of exact solution of example 5.2.1 with $M = N = 50$ 44

5.6 3D graph of error of example 5.2.1 44

List of Tables

5.1 L_∞ norm errors for example 5.2.1 when $M = 256$ and $r = \frac{2-\alpha}{\alpha}$ 39

5.2 L_∞ norm errors for example 5.1.1 when $M = 256$ and $r = 1$ 40

5.3 L_∞ norm errors for example 5.1.1 when $N = 10000$ 40

5.4 L_∞ norm errors for example 5.2.1 when $M = 256$ and $r = \frac{2-\alpha}{\alpha}$ 42

5.5 L_∞ norm errors for example 5.2.1 when $N = 5000$ 43

Table of Contents

Abstract **i**

List of Figures **ii**

List of Tables **iii**

1 Introduction **1**

1.1 Definitions and properties of fractional derivatives 1

1.1.1 Fractional integral 1

1.1.2 Caputo fractional derivative [4] 2

1.1.3 Some Properties 3

1.2 Numerical Techniques 3

1.3 Applications of the model problems: 5

2 Derivation of Numerical Methods **7**

2.1 Numerical method for non-linear time fractional equation 7

2.2 Numerical method for time fractional convection diffusion reaction equation with variable coefficients 12

3 Stability Analysis **20**

3.1 Stability analysis of numerical scheme of method (2.21)-(2.23) 20

3.2 Stability Analysis of numerical scheme of method (2.51)-(2.53) 23

4 Convergence Analysis **29**

4.1 Convergence analysis of method (2.21)-(2.23) 29

4.2 Convergence analysis of the method (2.51)-(2.53) 33

5 Numerical Results **38**

5.1 Numerical Illustration for TFBE 38

5.2 Numerical Illustration for TFFPE 42

6 Conclusion **45**

Bibliography **47**

Chapter 1

Introduction

Fractional calculus is a branch of mathematical analysis that studies the possibility of taking real-number powers of the differentiation operator $D = d/dx$ and the integration operator J, which generalizes the traditional integer-order calculus. Unlike its classical counterpart, fractional calculus incorporates the history of a process into its operators, providing a natural framework for modeling systems exhibiting memory and hereditary properties often observed in real-world applications. Stemming from inquiries into the meaning of non-integer order derivatives centuries ago, fractional calculus has evolved into a sophisticated field with significant theoretical advancements and a growing array of practical applications in various scientific domains. Increasingly, fractional differential equations (FDEs) are employed to model intricate physical and mechanical processes. They find widespread application across numerous fields, including anomalous diffusion, viscoelasticity, fluid mechanics, boundary layer analysis in pipelines, electromagnetism, signal and control theory, quantum economics, and fractal systems. Given that analytical solutions to FDEs are often unattainable, even for linear problems, the pursuit of reliable numerical methods constitutes an important direction in current research efforts.

1.1 Definitions and properties of fractional derivatives

1.1.1 Fractional integral

Definition 1.1.1 Suppose α is a positive real number and the function $f(x)$ is defined on the interval $[a, b]$. The α-th order fractional integral of the function $f(x)$ is defined

as

$$ {}_aD_s^{-\alpha} f(s) = \frac{1}{\Gamma(\alpha)} \int_a^s (s-\eta)^{\alpha-1} f(\eta) d\eta. \tag{1.1} $$

where $s \in$ [a,b] and $\Gamma(z)$ is the *Gamma* function defined by

$$ \Gamma(z) = \int_0^\infty \exp(-t) t^{z-1} dt, \quad Re(z) > 0. \tag{1.2} $$

1.1.2 Caputo fractional derivative [4]

Definition 1.1.2 Suppose α is a positive real number, $n-1 < \alpha < n$ with n a positive integer and the function $f^{(n)}(t)$ is continuous on the interval [a,b]. The α-th order **Caputo** fractional derivative of function $f(t)$ is defined as

$$ {}_a^C D_s^\alpha f(s) = \frac{1}{\Gamma(n-\alpha)} \int_a^s \frac{f^{(n)}(\eta) d\eta}{(s-\eta)^{\alpha-n+1}}, \tag{1.3} $$

where $s \in$ [a,b].
It can be easily shown that

$$ {}_a^C D_s^\alpha f(s) = {}_aD_s^{-(n-\alpha)} [f^{(n)}(s)]. \tag{1.4} $$

Assuming that the function $f(t)$, defined on the interval $[a, b]$, possesses continuous derivatives up to order $(n+1)$, then the following limit holds:

$$ \lim_{\alpha \to n} {}_a^C D_t^\alpha f(t) = \lim_{\alpha \to n} \left[\frac{f^{(n)}(a)(t-a)^{n-\alpha}}{\Gamma(n-\alpha+1)} + \frac{1}{\Gamma(n-\alpha+1)} \int_a^t (t-\tau)^{n-\alpha} f^{(n+1)}(\tau) d\tau \right] \tag{1.5} $$

Evaluating the limit on the right-hand side, this expression simplifies to:
$= f^{(n)}(a) + \int_a^t f^{(n+1)}(\tau) d\tau.$

By the Fundamental Theorem of Calculus, this is precisely the n-th derivative of $f(t)$:
$= f^{(n)}(t).$

1.1.3 Some Properties

- Non-Locality and Memory Effect:

  Unlike integer-order derivatives which are local operators (the derivative at a point depends only on the function's behavior in an arbitrarily small neighborhood of that point), fractional derivatives are generally non-local.

  The value of a fractional derivative at a given point depends on the history of the function over an interval leading up to that point. This "memory effect" allows fractional derivatives to naturally model processes with fading memory.

- Linearity:

  Fractional derivative obeys general linearity property ,i.e.,
  $D^{\alpha}(af(x) + e(x)) = aD^{\alpha}(f(x)) + D^{\alpha}(e(x))$. where a is any constant, $f(x)$ and $e(x)$ are functions, and D^{α} denotes the fractional derivative operator of order α.

1.2 Numerical Techniques

Various numerical techniques exist for approximating the Caputo fractional derivative, including the L1 formula, the L2-2σ formula, the L1-2σ formula, and the L2-1σ formula. In this study, we have chosen to employ the L1 formula for the discretization of the fractional derivative.

The L1 formula is generally a first-order method, meaning that the error of the approximation decreases linearly with the time step size (i.e., Error $\propto \tau$). However, the convergence order can be $(2-\alpha)$ if the solution f(t) has limited smoothness near $t = 0$, which is often the case for fractional differential equations.

In this thesis, we have explored and implemented numerical approach to find solutions for the following classes of equations:

1. *Time-Fractional Burgers' Equation (TFBE)*: For this equation, we employ the L1 scheme to handle the temporal discretization and the standard finite difference method (FDM) for the spatial discretization.

2. *Time-Fractional Fokker-Planck Equation (TFFPE)*: To solve this equation, we

utilized the L1 scheme for the time discretization and the Compact finite difference scheme (CFD) for the spatial discretization.

Now, we give some information about the compact finite difference scheme.
Compact finite difference methods are a class of numerical techniques which are used to approximate derivatives with high accuracy while using a minimal number of grid points (a small stencil). Unlike standard finite difference methods, CFD explicitly express derivatives based on neighboring function values and establish implicit relationships between the function values and their derivatives at adjacent points. This implicit nature is key to their enhanced performance.

Advantages of CFD Methods:

- *Higher Accuracy for Compact Stencils*: Achieves better accuracy with fewer computational points, potentially reducing computational cost and memory requirements.
- *Improved Resolution of Small Scales*: Better at capturing high-frequency components in the solution.
- *Better Stability Properties*: Often exhibit superior stability compared to explicit high-order FDM, especially for convection-dominated problems.
- *Favorable Wave Propagation Properties*: Lower dispersion and dissipation errors are crucial for accurate simulation of wave phenomena.

Disadvantages of CFD Methods:

- *Implicit Nature*: Requires solving a system of linear equations at each step (for derivatives) or each time level (for time-dependent problems), which adds computational overhead compared to explicit FDM.
- *Boundary Conditions*: Implementing boundary conditions for CFD schemes can be more complex than for explicit FDM, as the implicit relationships extend to the boundaries. Special treatment is often needed to maintain the desired accuracy.
- *Derivation Complexity*: Deriving high-order CFD schemes can be mathematically involved.

1.3 Applications of the model problems:

The TFBE, a generalization of the classical Burgers' equation, finds applications in modeling various physical phenomena where memory effects and non-local interactions play a significant role. Here are some key areas:

1. *Anomalous Diffusion*: The TFBE can describe sub-diffusive transport in porous media, where the rate of spread is slower than in normal diffusion due to other complex interactions within the medium.

2. *Viscoelasticity* [5]: It can model the behavior of viscoelastic materials that exhibit both viscous and elastic characteristics, where the material's response at a given time depends on its past deformation history.

3. *Fluid Flow* [6]: In fluid mechanics, the TFBE can be used to model certain types of non-Newtonian fluid flows or flows in complex geometries where fractional derivatives can capture deviations from standard viscous behavior. It has been applied to study shock propagation and boundary layer effects.

4. *Nonlinear Acoustics* [7]: The equation can describe the propagation of nonlinear acoustic waves in gas-filled pipes or other media where the wave behavior is influenced by both nonlinear advection and dissipative effects with memory.

5. *Contaminant Transport*: The TFBE can be employed to model the transport of contaminants in complex environments, such as groundwater, where anomalous diffusion due to the heterogeneous nature of the soil might occur.

The Time-Fractional Fokker-Planck Equation (TFFPE), a generalization of the classical Fokker-Planck equation, has found increasing utility in modeling complex phenomena across various scientific domains:

1. *Electromagnetism:* In certain electromagnetic systems, particularly those involving complex media or long-range interactions, the TFFPE can be used to model the time evolution of charged particle distributions and the associated

electromagnetic fields, offering insights beyond classical diffusion models.

2. *Quantum Economics and Finance:*

   The TFFPE is finding its way into economic and financial modeling [8] to describe phenomena that deviate from standard Brownian motion-based models. This includes capturing long-range dependencies, heavy tails in return distributions, and the impact of past information on current market behavior.

3. *Fractal Theory and Complex Systems:*

   Given its ability to model processes on fractal structures and systems with inherent memory, the TFFPE is a natural tool for studying complex systems across various disciplines, including physics, chemistry, and biology. It can describe transport and relaxation processes in these intricate environments.

4. *Biological Systems:* The TFFPE is increasingly used to model transport processes within biological cells [9], such as the movement of molecules in crowded cytoplasm or across membranes exhibiting anomalous diffusion. It can also describe the dynamics of biological populations and the spread of diseases with memory effects.

Chapter 2

Derivation of Numerical Methods

In this chapter, we derive numerical method for solving two time- fractional differential equations : (1) TFBE, (2) TFFPE.

2.1 Numerical method for non-linear time fractional equation

We consider the following nonlinear Time-Fractional Burgers' Equation (TFBE) equation [1]:

$$\begin{aligned} {}_0^C D_s^\alpha u(y,s) + u(y,s)u_y(y,s) - tu_{yy}(y,s) = L(y,s), \\ (y,s) \in (Y_l, Y_r) \times (0,S), \end{aligned} \tag{2.1}$$

where t embodies the viscosity parameter and $L(y,s)$ constitutes the source term. The initial condition (IC) is portrayed as

$$u(y,0) = f(y), \quad y \in [Y_l, Y_r] \tag{2.2}$$

and the boundary conditions (BCs) are portrayed as

$$u(Y_l,s) = \theta_1(s),\ u(Y_r,s) = \theta_2(s), \quad s \geqslant 0. \tag{2.3}$$

We consider sufficiently smooth functions $L(y,s)$, $f(y)$, $\theta_1(s)$, and $\theta_2(s)$.
The Caputo fractional derivative [4] for an order α, where $0 < \alpha < 1$, is defined as

$$ {}_0^C D_s^\alpha u(y,s) = \frac{1}{\Gamma(1-\alpha)} \int_0^s (s-t)^{-\alpha} \frac{\partial u(y,t)}{\partial t} dt. \tag{2.4}$$

We'll develop a numerical method to find solutions for the (TFBE) given by (2.1), satisfying IC stated in (2.2) and BCs provided in (2.3).

- **TIME DISCRETIZATION**

  We discretize the time variable of the problem defined by equations (2.1)-(2.3) on the interval $[0, S]$. To achieve this, we introduce a graded mesh, $\mathscr{D}_1 = \{s_0 = 0, s_1, \ldots, s_N = S\}$ with mesh size $\tau_n = s_n - s_{n-1}$ for $n = 1, 2, 3, \ldots, N-1$, where $N > 1$ represents an integer. We define $s_n = S(n/N)^r$ for $n = 1, 2, 3, \ldots, N$,where $r \geqslant 1$ embodies a mesh grading constant.

  Subsequently, the Caputo fractional derivative, as defined in Equation (2.4), can be discretized using the L1 scheme [3] in the following manner:

$$\begin{aligned}
{}_0^C D_s^\alpha u(y,s_n) &= \frac{1}{\Gamma(1-\alpha)} \int_0^{s_n} (s_n - t)^{-\alpha} \frac{\partial u(y,t)}{\partial t} dt \\
&= \frac{1}{\Gamma(1-\alpha)} \sum_{j=0}^{n-1} \int_{s_j}^{s_{j+1}} (s_n - t)^{-\alpha} \frac{\partial u(y,t)}{\partial t} dt \\
&= \frac{1}{\Gamma(1-\alpha)} \sum_{j=0}^{n-1} \frac{u(y,s_{j+1}) - u(y,s_j)}{s_{j+1} - s_j} \int_{s_j}^{s_{j+1}} (s_n - t)^{-\alpha} dt + \mathcal{R}_1^n \\
&= \frac{1}{\Gamma(2-\alpha)} \sum_{j=0}^{n-1} \frac{u(y,s_{j+1}) - u(y,s_i)}{\tau_i} [(s_n - s_j)^{1-\alpha} - (s_n - s_{j+1})^{1-\alpha}] + \mathcal{R}_1^n \\
&= {}_0^C D_N^\alpha u(y,s_n) + \mathcal{R}_1^n.
\end{aligned} \tag{2.5}$$

  The discretization of the Caputo derivative using the L1 scheme introduces a truncation error, denoted as $\mathcal{R}_1^n$. This error is bounded by [3]:

$$|\mathcal{R}_1^n| \leqslant \mathcal{C}_1 n^{-min\{2-\alpha, r\alpha\}}. \tag{2.6}$$

Equation (2.1) at the time point $s = s_n$ leads to

$$ {}_0^C D_s^\alpha u(y, s_n) + u(y, s_n) u_y(y, s_n) - t u_{yy}(y, s_n) = L(y, s_n), \tag{2.7} $$

IC:

$$ u(y, s_0) = f(y), \quad y \in [Y_l, Y_r], $$

BCs:

$$ u(Y_l, s_n) = \theta_1(s_n), $$

$$ u(Y_r, s_n) = \theta_2(s_n). $$

By means of (2.5) and denoting $u(y, s_n) = u^n(y)$, we obtain:

$$ \begin{aligned} &\frac{1}{\Gamma(2-\alpha)} \sum_{j=0}^{n-1} \frac{u^{j+1}(y) - u^j(y)}{s_{j+1} - s_j} [(s_n - s_j)^{1-\alpha} - (s_n - s_{j+1})^{1-\alpha}] \\ &+ (u u_y)^n(y) - t u_{yy}^n(y) = L^n(y) + \mathcal{R}_1^n. \end{aligned} \tag{2.8} $$

To handle the nonlinear term $(uu_y)^n(y)$, we employ a linearization technique [10], resulting in the following approximation:

$$ (u u_y)^n(y) = u^n u_y^{n-1}(y) + u^{n-1} u_y^n(y) - (u u_y)^{n-1}(y) \tag{2.9} $$

Substituting the linearized form of $(uu_y)^n(y)$, we obtain the semi- discretized equation for Equation (2.1), as follows

$$ \begin{aligned} &\frac{1}{\Gamma(2-\alpha)} \sum_{j=0}^{n-1} \frac{u^{j+1}(y) - u^j(y)}{s_{j+1} - s_j} [(s_n - s_j)^{1-\alpha} - (s_n - s_{j+1})^{1-\alpha}] \\ &+ u^n u_y^{n-1}(y) + u^{n-1} u_y^n(y) - (u u_y)^{n-1}(y) - t u_{yy}^n(y) = L^n(y) + \mathcal{R}_1^n. \end{aligned} \tag{2.10} $$

- **SPACE DISCRETIZATION**

  Moving on to the spatial discretization, we now apply the standard FDM to

equation (2.10). For this, we define a uniform spatial mesh $\mathscr{D}_2 = \{Y_l = y_0, y_1, \ldots, y_M = Y_r\}$, where the spatial nodes are given by $y_m = mh, m = 0, 1, 2, 3, \ldots, M$ and h denotes the uniform step size in the spatial direction.

The second-order central finite difference approximation for the second order spatial derivative $u_{yy}(y_m)$ is given by:

$$u_{yy}(y_m) = \frac{u(y_{m+1}) - 2u(y_m) + u(y_{m-1})}{h^2} - q_1, \quad m = 1, \ldots, M-1, \tag{2.11}$$

where

$$q_1 = \frac{h^2}{12}u^{(4)}(y_m) + \mathcal{O}(h^4), \quad m = 1, \ldots, M-1. \tag{2.12}$$

Similarly, the second-order central finite difference approximation for the first order spatial derivative $u_y(y_m)$ is expressed as:

$$u_y(y_m) = \frac{u(y_{m+1}) - u(y_{m-1})}{2h} - q_2, \quad m = 1, \ldots, M-1, \tag{2.13}$$

where

$$q_2 = \frac{h^2}{6}u^{(3)}(y_m) + \mathcal{O}(h^4), \quad m = 1, \ldots, M-1. \tag{2.14}$$

At $y = y_m$ equation (2.10) becomes:

$$\begin{aligned} &\frac{1}{\Gamma(2-\alpha)}\sum_{j=0}^{n-1}\frac{u^{j+1}(y_m) - u^i(y_m)}{s_{j+1} - s_j}[(s_n - s_j)^{1-\alpha} - (s_n - s_{j+1})^{1-\alpha}] \\ &\quad + u^n u_y^{n-1}(y_m) + u^{n-1}u_y^n(y_m) - (uu_y)^{n-1}(y_m) - tu_{yy}^n(y_m) \\ &= L^n(y_m) + \mathcal{R}_1^n. \end{aligned} \tag{2.15}$$

We denote $u(y_m)^n = u_m^n$ in the above equation to get

$$\begin{aligned} &\frac{1}{\Gamma(2-\alpha)}\sum_{j=0}^{n-1}\frac{(u_m^{j+1} - u_m^j)}{s_{j+1} - s_i}[(s_n - s_i)^{1-\alpha} - (s_n - s_{j+1})^{1-\alpha}] \\ &+u_m^n(u_y)_m^{n-1} + u_m^{n-1}(u_y)_m^n - (uu_y)_m^{n-1} - t(u_{yy})_m^n = L_m^n + \mathcal{R}_1^n. \end{aligned} \tag{2.16}$$

Now, by substituting the finite difference approximations from equation (2.11)

and equation (2.13) into equation (2.16),
we obtain the fully discretized form of equation (2.1):

$$\begin{aligned}
&-t\left(\frac{u_{m+1}^{n}-2u_{m}^{n}+u_{m-1}^{n}}{h^{2}}\right)\\
&\quad+\frac{u_{m}^{n}u_{m+1}^{n-1}-u_{m}^{n}u_{m-1}^{n-1}+u_{m}^{n-1}u_{m+1}^{n}-u_{m}^{n-1}u_{m-1}^{n}-u_{m}^{n-1}u_{m+1}^{n-1}+u_{m}^{n-1}u_{m-1}^{n-1}}{2h}\\
&\quad=L_{m}^{n}-\frac{1}{\Gamma(2-\alpha)}\sum_{j=0}^{n-1}\frac{u_{m}^{j+1}-u_{m}^{j}}{s_{j+1}-s_{j}}[(s_{n}-s_{j})^{1-\alpha}-(s_{n}-s_{j+1})^{1-\alpha}]\\
&\qquad+(\mathcal{R}_{1})_{m}^{n}+(\mathcal{R}_{2})_{m}^{n}.
\end{aligned}\tag{2.17}$$

The spatial discretization introduces a truncation error at the node $y = y_m$ and time step $s = s_n$ denoted by $(\mathcal{R}_2)_m^n$, which is bounded by:

$$|(\mathcal{R}_{2})_{m}^{n}|\leqslant\mathcal{C}_{2}(h^{2}).\tag{2.18}$$

Combining the truncation errors from both the temporal and spatial discretizations, we obtain the total truncation error as:

$$\begin{aligned}
&\frac{u_{m}^{n}u_{m+1}^{n-1}-u_{m}^{n}u_{m-1}^{n-1}+u_{m}^{n-1}u_{m+1}^{n}-u_{m}^{n-1}u_{m-1}^{n}-u_{m}^{n-1}u_{m+1}^{n-1}+u_{m}^{n-1}u_{m-1}^{n-1}}{2h}\\
&\quad-t\left(\frac{u_{m+1}^{n}-2u_{m}^{n}+u_{m-1}^{n}}{h^{2}}\right)\\
&=L_{m}^{n}-\frac{1}{\Gamma(2-\alpha)}\sum_{j=0}^{n-1}\frac{u_{m}^{j+1}-u_{m}^{j}}{s_{j+1}-s_{j}}[(s_{n}-s_{j})^{1-\alpha}-(s_{n}-s_{j+1})^{1-\alpha}]+\mathcal{R}_{m}^{n}.
\end{aligned}\tag{2.19}$$

Therefore, the total truncation error $\mathcal{R}_m^n$ is bounded by:

$$|\mathcal{R}_{m}^{n}|\leqslant\mathcal{C}(h^{2}+n^{-\min\{2-\alpha,r\alpha\}}).\tag{2.20}$$

By disregarding the truncation error term $\mathcal{R}_m^n$, we arrive at the following numerical

scheme that approximates the solution of the original problem:

$$\left(\frac{-t}{h^2}-\frac{U_m^{n-1}}{2h}\right)U_{m-1}^n+\left(\frac{2t}{h^2}+\frac{U_{m+1}^{n-1}-U_{m-1}^{n-1}}{2h}+\frac{1}{\Gamma(2-\alpha)(s_n-s_{n-1})^\alpha}\right)U_m^n$$
$$+\left(\frac{-t}{h^2}+\frac{U_m^{n-1}}{2h}\right)U_{m+1}^n=L_m^n-\frac{U_m^{n-1}U_{m-1}^{n-1}-U_m^{n-1}U_{m+1}^{n-1}}{2h}$$
$$-\left(\sum_{j=0}^{n-2}\frac{(U_m^{j+1}-U_m^j)\{(s_n-s_j)^{1-\alpha}-(s_n-s_{j+1})^{1-\alpha}\}}{(s_{j+1}-s_j)\Gamma(2-\alpha)}\right)+\frac{U_m^{n-1}}{(s_n-s_{n-1})^\alpha\Gamma(2-\alpha)}. \tag{2.21}$$

$m=1,2,3,...,M-1$ and $n=1,2,...,N$,

$$U_m^0=f(y_m), m=1,2,3,...M, \tag{2.22}$$

$$U_0^n=\theta_1(s_n), U_M^n=\theta_2(s_n), n=1,2,3,...,N \tag{2.23}$$

In this numerical scheme, U_m^n represents the numerical approximation of the exact solution $U(x_m,t_n)$ at the spatial node y_m and the time step t_n, and L_m^n denotes the value of the function at (y_m,s_n).

2.2 Numerical method for time fractional convection diffusion reaction equation with variable coefficients

We consider the following TFFP equation [2]:

$$\begin{aligned}{}_0^C D_s^\alpha u(y,s)+P(y)u_y(y,s)-u_{yy}(y,s)+P'(y)u(y,s)=L(y,s),\\ (y,s)\in(Y_l,Y_r)\times(0,S),\end{aligned} \tag{2.24}$$

where $L(y,s)$ denotes the source term . The initial condition is portrayed as

$$u(y,0)=f(y),\quad y\in[Y_l,Y_r] \tag{2.25}$$

and the boundary conditions are portrayed as

$$u(Y_l,s)=\theta_1(s),\ u(Y_r,s)=\theta_2(s),\quad s\geqslant 0. \tag{2.26}$$

We consider sufficiently smooth functions $L(y,s)$, $f(y)$, $\theta_1(s)$, and $\theta_2(s)$. In this section, we will focus on developing a numerical scheme to solve the TFFP equation given by (2.24), while adhering to the IC provided in (2.25) and the Boundary Conditions specified in (2.26).

- **TIME DISCRETIZATION**

  We discretize the time variable of the problem defined by equations (2.24)-(2.26) on the interval $[0,S]$. To achieve this, we introduce a graded mesh denoted by $\mathscr{D}_1 = \{s_0 = 0, s_1, \ldots, s_N = S\}$, where N>1 represents an integer. The time step size is given by $\tau_n = s_n - s_{n-1}$ for $n = 1,2,3,\ldots,N-1$. The time points t_n are specifically defined as $t_n = S(n/N)^r$ for $n = 1,2,3,\ldots,N$ with $r \geqslant 1$, being a parameter that controls the grading of the mesh.

  Subsequently, the Caputo fractional derivative, as defined in Equation (2.4), can be discretized using the L1 scheme, as detailed in reference [3], in the following manner:

$$
\begin{aligned}
&{}_0^C D_s^\alpha u(y,s_n) \\
&= \frac{1}{\Gamma(1-\alpha)} \int_0^{s_n} (s_n - t)^{-\alpha} \frac{\partial u(y,t)}{\partial t} dt \\
&= \frac{1}{\Gamma(1-\alpha)} \sum_{j=0}^{n-1} \int_{s_j}^{s_{j+1}} (s_n - t)^{-\alpha} \frac{\partial u(y,t)}{\partial t} dt \\
&= \frac{1}{\Gamma(1-\alpha)} \sum_{j=0}^{n-1} \frac{u(y,s_{j+1}) - u(y,s_j)}{s_{j+1} - s_j} \int_{s_j}^{s_{j+1}} (s_n - t)^{-\alpha} dt + \mathcal{R}_1^n \\
&= \frac{1}{\Gamma(2-\alpha)} \sum_{j=0}^{n-1} \frac{u(y,s_{j+1}) - u(y,s_j)}{\tau_n} [(t_n - t_i)^{1-\alpha} - (s_n - s_{j+1})^{1-\alpha}] + \mathcal{R}_1^n \\
&= {}_0^C D_N^\alpha v(y,s_n) + \mathcal{R}_1^n,
\end{aligned}
\tag{2.27}
$$

  where the truncation error $\mathcal{R}_1^n$ has following bound :

$$
|\mathcal{R}_1^n| \leqslant \mathcal{C}_1 n^{-\{2-\alpha\}}. \tag{2.28}
$$

At the time point $s = s_n$, equation (2.24) This yields:

$$ {}_0^C D_s^\alpha u(y, s_n) + P(y)u_y(y, s_n) + P'(y)u(y, s_n) - u_{yy}(y, s_n) = L(y, s_n), \tag{2.29} $$

IC:

$$ u(y, s_0) = f(y), \quad y \in [Y_l, Y_r], $$

BCs:

$$ u(Y_l, s_n) = \theta_1(s_n), $$

$$ u(Y_r, s_n) = \theta_2(s_n). $$

We denote $u(y, s_n)$ by $u^n(y)$ and using (2.27) in (2.29), we get the following discretized form of equation (2.24) in time direction:

$$ \begin{aligned} &\frac{1}{\Gamma(2-\alpha)} \sum_{j=0}^{n-1} \frac{u^{j+1}(y) - u^j(y)}{s_{j+1} - s_j} [(s_n - s_j)^{1-\alpha} - (s_n - s_{j+1})^{1-\alpha}] \\ &+ P(y)(u_y)^n(y) + P'(y)u^n(y) - u_y^n(y) = L^n(y) + \mathcal{R}_1^n. \end{aligned} \tag{2.30} $$

with **IC:**

$$ u(y, s_0) = u_y^0 = f(y), \quad Y_l < y < Y_r, \tag{2.31} $$

and the **BCs:**

$$ \begin{aligned} u(Y_l, s_n) = u^n(s_n) = \theta_1(Y_l, s_n), \\ u(Y_r, s_n) = u^n(s_n) = \theta_2(Y_l, s_n), n \geqslant 1. \end{aligned} \tag{2.32} $$

- **SPACE DISCRETIZATION**

  Consider the semi-discretized equation (2.30), along with its initial Ccndition (2.31) and boundary conditions (2.32), we apply the CFD for spatial discretization. To do this, we define a uniform partition of the spatial domain $[Y_l, Y_r]$ as$Y_l \equiv y_0 < y_1, ... < y_m < y_{m+1} < ... < y_M \equiv Y_r$, where M is a positive integer

and the step size is uniform, given by $h = (y_m - y_{m-1}), m = 1, 2, .., M$.

The standard second-order finite difference approximation for the second spatial derivative $u_{yy}(y_m)$ is given by:

$$u_{yy}(y_m) = \frac{u(y_{m+1}) - 2u(y_m) + u(y_{m-1})}{h^2} - q_1, \quad m = 1, \ldots, M-1, \tag{2.33}$$

where

$$q_1 = \frac{h^2}{12} u^{(4)}(y_m) + \mathcal{O}(h^4), \quad m = 1, \ldots, M-1. \tag{2.34}$$

For $u_y(y_m)$, the second order finite difference approximation is given by

$$u_y(y_m) = \frac{u(y_{m+1}) - u(y_{m-1})}{2h} - q_2, \quad m = 1, \ldots, M-1, \tag{2.35}$$

where

$$q_2 = \frac{h^2}{6} u^{(3)}(y_m) + \mathcal{O}(h^4), \quad m = 1, \ldots, M-1. \tag{2.36}$$

Our objective is to achieve a higher accuracy in the spatial approximation, specifically aiming for a fourth-order approximation of the solution for the problem at hand. To accomplish this, we will first develop a CFD scheme that provides a fourth-order accuracy for a general differential equation of the form:

$$-u''(y) + P_1(y)u'(y) + P_1'(y)u(y) = F(y). \tag{2.37}$$

Using (2.30),(2.33) and (2.35), the finite discretized form of (2.37) at $y = y_m$ is given by

$$-\delta_y^2 u(y_m) + P_1(y_m)\delta_y u(y_m) + P_1'(y_m)u(y_m) - Q = F(y_m). \tag{2.38}$$

where

$$Q = \frac{h^2}{6}P_1(y_m)u^{(3)}(y_m) - \frac{h^2}{12}u^{(4)}(y_m) + \frac{h^4}{120}P_1(y_m)u^{(5)}(y_m) - \frac{h^4}{360}u^{(6)}(y_m) + \mathcal{O}(h^6). \tag{2.39}$$

We differentiate (2.37) with respect to y, in order to approximate $u^{(3)}(y_m)$ and $u^{(4)}(y_m)$ in (2.39). Another change we can do from here is that replace $P_1'(y)$ by $R(y)$. Thus, for $y = y_m$, we have

$$u^{(3)}(y_m) = P_1(y_m)u''(y_m) + (R(y_m) + P_1'(y_m))u'(y_m) + R'(y_m)u(y_m) - F'(y_m) \tag{2.40}$$

Differentiating (2.37) twice with respect to y at $y = y_m$, we have

$$\begin{aligned} u^{(4)}(y_m) = {} & (P_1(y_m)^2 + 2P_1'(y_m) + R(y_m))u''(y_m) \\ & + (P_1(y_m)P_1'(y_m) + P_1(y_m)R(y_m) + P_1''(y_m) + 2R'(y_m))u'(y_m) \\ & + (P_1(y_m)R'(y_m) + R''(y_m))u(y_m) \\ & + (-F''(y_m) - P_1(y_m)F'(y_m)). \end{aligned} \tag{2.41}$$

Substituting (2.40) and (2.41) into (2.39), we have

$$\begin{aligned} Q = -\frac{h^2}{12}\Bigg[& (-P_1(y_m)^2 + 2P_1'(y_m) + R(y_m))\delta_y^2 u(y_m) \\ & + (-P_1(y_m)P_1'(y_m) - P_1(y_m)R(y_m) + P_1''(y_m) + 2R'(y_m))\delta_y u(y_m) \\ & + (-P_1(y_m)R'(y_m) + R''(y_m))u(y_m) \\ & + (-\delta_y^2 F(y_m) + P_1(y_m)\delta_y F(y_m))\Bigg] + \mathcal{T}. \end{aligned} \tag{2.42}$$

where

$$\begin{aligned} \mathcal{T} = -\frac{h^4}{144}\Bigg[& (P_1(y_m)^2 - 2P_1'(y_m) - R(y_m))u^{(4)}(y_m) \\ & + (2P_1(y_m)P_1'(y_m) + 2P_1(y_m)R(y_m) - 2P_1''(y_m) + 4R'(y_m))u^{(3)}(y_m) \\ & + (F^{(4)}(y_m) - 2P_1(y_m)F^{(3)}(y_m))\Bigg] + \mathcal{O}(h^6). \end{aligned} \tag{2.43}$$

By substituting (2.42) in (2.38), we draw

$$\begin{aligned}
&\left(-1 + \frac{h^2}{12}(-P_1(y_m)^2 + 2P_1'(y_m) + R(y_m)) \right)\delta_y^2 u(y_m) \\
&+ \left(P_1(y_m) + \frac{h^2}{12}(-P_1(y_m)P_1'(y_m) - P_1(y_m)R(y_m) + P_1''(y_m) + 2R'(y_m)) \right)\delta_y u(y_m) \\
&+ \left(R(y_m) + \frac{h^2}{12}(-P_1(y_m)R'(y_m) + R''(y_m)) \right)u(y_m) \\
&= F(y_m) - \frac{h^2}{12}(-\delta_x^2 F(y_m) + P_1(y_m)\delta_y F(y_m)) + \mathcal{R}_2^m.
\end{aligned} \tag{2.44}$$

where $|\mathcal{R}_2^m| \leqslant \mathcal{C}_2(h^4)$ for a positive constant $\mathcal{C}_2$.
Now, assume $v(y,s) = {}_0^C D_s^\alpha u(y,s)$. For the point (y_m, s_n), we draw $v(y_m, s_n) = {}_0^C D_N^\alpha u(y_m, s_n)$. Hence, we have,

$$w(y_m, s_n) = \frac{1}{\Gamma(2-\alpha)} \sum_{j=0}^{n-1} \frac{u_m^{j+1} - u_m^j}{s_{j+1} - s_j}[(s_n - s_j)^{1-\alpha} - (s_n - s_{j+1})^{1-\alpha}] + \mathcal{R}^n. \tag{2.45}$$

Considering (2.30) at $y = y_m$, we draw

$$-u_{yy}(y_m, s_n) + P_1(y_m)u_y(y_m, s_n) - R(y_m, s_n) = L(y_m, s_n) - w(y_m, s_n). \tag{2.46}$$

By employing the relationships derived in (2.44), we can establish the following fourth-order compact finite difference scheme for the equation (2.46):

$$\begin{aligned}
&\left(-1 + \frac{h^2}{12}(-P_1(y_m)^2 + 2P_1'(y_m) + R(y_m)) \right)\delta_y^2 u(y_m) \\
&+ \left(P_1(y_m) + \frac{h^2}{12}(-P_1(y_m)P_1'(y_m) - P_1(y_m)R(y_m) + P_1''(y_m) + 2R'(y_m)) \right)\delta_y u(y_m) \\
&+ \left(R(y_m) + \frac{h^2}{12}(-P_1(y_m)R'(y_m) + R''(y_m)) \right)u(y_m) \\
&= L(y_m, s_n) - w(y_m, s_n) - \frac{h^2}{12}(-\delta_y^2(L(y_m, s_n) - w(y_m, s_n)) \\
&\quad + P_1(y_m)\delta_y(L(y_m, s_n) - w(y_m, s_n))) + \mathcal{R}_n^m,
\end{aligned} \tag{2.47}$$

where

$$\mathcal{R}_m^n = \left(1 + \frac{h^2}{12}(\delta_y^2 - P_1(y_m)\delta_y)\right)\mathcal{R}_1^n + \mathcal{R}_2^m \tag{2.48}$$

and the truncation error $\mathcal{R}_m^n$ has following bound:

$$|\mathcal{R}_m^n| \quad \leqslant \mathcal{C}(h^4 + n^{-\{2-\alpha\}}). \tag{2.49}$$

Thus, the higher-order compact finite difference scheme for the Time-Fractional Fokker-Planck (TFFP) equation (2.24) subject to the initial Condition (2.25) and boundary conditions (2.26) can be expressed as follows:

$$\begin{aligned} \mathcal{H}_m \frac{v(y_m, s_n)}{\Gamma(2-\alpha)} - \mathcal{A}_m \delta_x^2 u(y_m, s_n) + \mathcal{C}_m \delta_y u(y_m, s_n) \\ + \mathcal{H}_m R(y_m) u(y_m, s_n) = \mathcal{H}_m L(y_m, s_n) + \mathcal{R}_m^n; \\ 1 \leqslant m \leqslant M-1, \quad 1 \leqslant n \leqslant N; \end{aligned} \tag{2.50}$$

$$\textbf{BC:} u(0, s_n) = \theta_1(0, s_n) \quad u(M, s_n) = \theta_2(M, s_n); \quad 1 \leqslant n \leqslant N; \tag{2.51}$$

$$\textbf{IC:} u(y_m, 0) = f(y_m); \quad 0 \leqslant m \leqslant M; \tag{2.52}$$

where

$\mathcal{H}_m = 1 + \frac{h^2}{12}(\delta_y^2 - P_1(y_m)\delta_y), \mathcal{A}_m = 1 + \frac{h^2}{12}(P_1(y_m)^2 - 2\delta_y P_1(y_m)), \mathcal{C}_m = P_1(y_m) + \frac{h^2}{12}(\delta_y^2 P_1(y_m) - P_1(y_m)\delta_y P_1(y_m))$.

Denoting $u(y_m, s_n) = u_m^n$ and v_m^n as the approximated solution of u_m^n and deleting the truncation error term from (2.29), we obtains the following numerical scheme for the problem (2.24)-(2.26):

$$
\begin{aligned}
v_{m-1}^{n}\Bigg(& -\frac{1}{h^2}+\frac{2(P_1')_m+R_m-(P_1)_m^2}{12}-\frac{(P_1)_m}{2h} \\
& -\frac{h((P_1)_m''-(P_1)_m(P_1')_m-(P_1)_mR_m+2(P_2')_m)}{24} \\
& +\frac{((s_n-s_{n-1})^{-\alpha})(2+(P_1)_mh)}{24\Gamma(2-\alpha)}\Bigg) \\
& +v_m^n\Bigg(\frac{2}{h^2}-\frac{2(P_1')_m+R_m-(P_1)_m^2}{6}+(P_2)_m+\frac{h^2(R_m''-(P_1)_mR_m)}{12} \\
& +\frac{5((s_n-s_{n-1})^{-\alpha})}{6\Gamma(2-\alpha)}\Bigg)+v_{m+1}^n\Bigg(-\frac{1}{h^2}+\frac{2(P_1')_m+R_m-(P_1)_m^2}{12}+\frac{(P_1)_m}{2h} \\
& +\frac{h((P_1)_m''-(P_1)_m(P_1')_m-(P_1)_mR_m+2(P_2')_m)}{24} \\
& +\frac{((s_n-s_{n-1})^{-\alpha})(2-(P_1)_mh)}{24\Gamma(2-\alpha)}\Bigg) \\
& =\frac{(2-(P_1)_mh)L_{m+1}^n+10L_m^n+(2+(P_1)_mh)L_{m-1}^n}{24} \\
& +\frac{1}{\Gamma(2-\alpha)}\sum_{j=0}^{n-2}\frac{(s_n-s_j)^{1-\alpha}-(s_n-s_{j+1})^{1-\alpha})}{s_{j+1}-s_j} \\
& \quad\times\Bigg((v_{m-1}^{j+1}-v_{m-1}^{j})\left(\frac{-2-(P_1)_mh}{24}\right)+(v_m^{j+1}-v_m^j)(-5/6) \\
& +(v_{m+1}^{j+1}-v_{m+1}^{j})\left(\frac{-2+(P_1)_mh}{24}\right)\Bigg)-\frac{(s_n-s_{n-1})^{-\alpha}}{\Gamma(2-\alpha)} \\
& \left(v_{m-1}^{n-1}\left(\frac{-2-(P_1)_mh}{24}\right)+v_m^{n-1}(-5/6)+v_{m+1}^{n-1}\left(\frac{-2+(P_1)_mh}{24}\right)\right).
\end{aligned}
\tag{2.53}
$$

Chapter 3

Stability Analysis

In this chapter, we provide stability results of the proposed methods.

3.1 Stability analysis of numerical scheme of method (2.21)-(2.23)

In this section, we will process stability analysis of the numerical method defined by (2.21)-(2.23). Let

$$\zeta_m^n = U_m^n - V_m^n \tag{3.1}$$

where, U_m^n is the approximate solution of V_m^n. Using equation (3.1) to the error term ζ_m^n, we derive the following expression for the round-off error equation:

$$\begin{aligned}\left(\frac{-t}{h^2} - \frac{\zeta_m^{n-1}}{2h}\right)\zeta_{m-1}^n + \left(\frac{2v}{h^2} + \frac{\zeta_{m+1}^{n-1} - \zeta_{m-1}^{n-1}}{2h} + \frac{1}{\Gamma(2-\alpha)(s_n - s_{n-1})^\alpha}\right)\zeta_m^n \\ + \left(\frac{-t}{h^2} + \frac{\zeta_m^{n-1}}{2h}\right)\zeta_{m+1}^n = -\frac{\zeta_m^{n-1}\zeta_{m-1}^{n-1} - \zeta_m^{n-1}\zeta_{m+1}^{n-1}}{2h} \\ -\left(\sum_{j=0}^{n-2} \frac{(\zeta_m^{j+1} - \zeta_m^j)\{(s_n - s_j)^{1-\alpha} - (s_n - s_{j+1})^{1-\alpha}\}}{(s_{j+1} - s_j)(\Gamma(2-\alpha))}\right) + \frac{\zeta_m^{n-1}}{(s_n - s_{n-1})^\alpha(\Gamma(2-\alpha))},\end{aligned} \tag{3.2}$$

The modified representation of equation (3.2) is as follows:

$$\left(\frac{-t}{h^2}-\frac{\zeta_m^{n-1}}{2h}\right)\zeta_{m-1}^n+\left(\frac{2v}{h^2}+\frac{\zeta_{m+1}^{n-1}-\zeta_{m-1}^{n-1}}{2h}+w\right)\zeta_m^n+\left(\frac{-t}{h^2}+\frac{\zeta_m^{n-1}}{2h}\right)\zeta_{m+1}^n$$
$$=-\frac{\zeta_m^{n-1}\zeta_{m-1}^{n-1}-\zeta_m^{n-1}\zeta_{m+1}^{n-1}}{2h}+w\left(\sum_{j=1}^{n-1}\zeta_m^{n-j}(b_{j-1}-b_j)+b_{n-1}\zeta_0\right), \tag{3.3}$$

$m=1,2,3,...,M-1, n=1,2,3,...,N,$

where $w=\frac{(s_n-s_{n-1})^{1-\alpha}}{\Gamma(2-\alpha)}$ and $b_j=(j+1)^{1-\alpha}-(j)^{1-\alpha}$.

Define a grid function $\zeta^n(y)$ for $n=1,2,3,...,N$ as

$$\zeta^n(y)=\begin{cases}\zeta_m^n, & \text{if} \quad y\in(y_{m-\frac{1}{2}},y_{m+\frac{1}{2}}], m=1,2,...,M-1,\\ 0, & \text{if} \quad y\in[0,\frac{h}{2}]\cup(1-\frac{h}{2},1]\end{cases} \tag{3.4}$$

and let $\zeta^n=[\zeta_1^n,\zeta_2^n,...,\zeta_{M-1}^n]^T$. Define the following norm

$$\parallel\zeta^n\parallel_2=\left(\sum_{m=1}^{M-1}h\mid\zeta_m^n\mid^2\right)^{\frac{1}{2}}=\left(\sum_{-\infty}^{\infty}\mid\zeta_n(l)\mid^2\right)^{\frac{1}{2}}, n=0,1,2,...,N, \tag{3.5}$$

where $\zeta_n(l)$ is the Fourier coefficient (FC) of the series for $\zeta^n(y)$. We write ζ_m^n in the following form

$$\zeta_m^n=\xi_n e^{\iota m\rho h}, \tag{3.6}$$

where $\iota=\sqrt{-1}$. Inserting (3.6) in (3.3) gives

$$\xi_n e^{\iota m\rho h}\left[\left(\frac{-t}{h^2}-\frac{\xi_{n-1}e^{\iota m\rho h}}{2h}\right)e^{-\iota\rho h}+\left(\frac{2t}{h^2}+\frac{\xi_{n-1}e^{\iota m\rho h}(e^{\iota\rho h}-e^{-\iota\rho h})}{2h}+w\right)\right.$$
$$\left.+\left(\frac{-t}{h^2}+\frac{\xi_{n-1}e^{\iota m\rho h}}{2h}\right)e^{\iota\rho h}\right]=e^{\iota m\rho h}\left[-\frac{\xi_{n-1}(e^{\iota(m-1)\rho h}-e^{\iota(m+1)\rho h})}{2h}\right. \tag{3.7}$$
$$\left.+w\left(\sum_{j=1}^{n-1}\xi_{n-j}(b_{j-1}-b_j)+b_{n-1}\xi_0\right)\right].$$

Equation (3.7) is equivalent to

$$\xi_n\left[\left(-\frac{2t\cos\rho h}{h^2}+\frac{\iota\sin\rho h(\xi_{n-1}e^{\iota m\rho h})}{h}\right)+\left(\frac{2t}{h^2}+\frac{\iota\sin\rho h(\xi_{n-1}e^{\iota m\rho h})}{h}\right)+w\right] = \left[\frac{\iota\xi_{n-1}(e^{\iota m\rho h})\sin\rho h}{h}+w\left(\sum_{j=1}^{n-1}\xi_{n-j}(b_{j-1}-b_j)+b_{n-1}\xi_0\right)\right]. \tag{3.8}$$

Equation (3.8) implies that

$$\xi_n=\frac{\left[\frac{\iota\xi_{n-1}(e^{\iota m\rho h})\sin\rho h}{h}+w\left(\sum_{j=1}^{n-1}\xi_{n-j}(b_{j-1}-b_j)+b_{n-1}\xi_0\right)\right]}{\left[w+\frac{4v(\sin^2\rho h)}{h^2}+\frac{2\iota\xi_{n-1}(e^{\iota m\rho h})\sin\rho h}{h}\right]} \tag{3.9}$$

$$|\,\xi_n\,| \quad \leq \quad \sum_{j=1}^{n-1}|\,\xi_{n-j}\,|\,(b_{j-1}-b_j)+b_{n-1}\,|\,\xi_0\,|\,. \tag{3.10}$$

Theorem The present method (2.21-2.23) for TFBEs (2.1–2.3) is unconditionally stable.

Proof We firstly show that

$$|\,\xi_n\,|\leq|\,\xi_0\,|\,. \tag{3.11}$$

We prove this result by mathematical induction. Setting $n=1$ in (3.10) yields

$$|\,\xi_1\,| \quad \leq \quad b_0\,|\,\xi_0\,|\,. \tag{3.12}$$

Since $b_0=1$, from equation (3.12), we get

$$|\,\xi_1\,| \quad \leq \quad |\,\xi_0\,|\,. \tag{3.13}$$

Therefore, (3.11) is valid for $n=1$. In view of the principle of mathematical induction, suppose that (3.11) is valid for $n\leq k-1$. i.e.

$$|\,\xi_n\,| \quad \leq \quad |\,\xi_0\,|, n=1,2,...,(k-1). \tag{3.14}$$

For $n = k$, (3.10) becomes

$$| \xi_k | \quad \leq \quad \sum_{j=1}^{n-1} | \xi_{k-j} | (b_{j-1} - b_j) + b_{k-1} | \xi_0 | . \tag{3.15}$$

Inserting (3.14) into (3.15), we obtain

$$| \xi_k | \quad \leq \quad \sum_{j=1}^{n-1} | \xi_0 | (b_{j-1} - b_j) + b_{k-1} | \xi_0 | \quad \leq \quad b_0 | \xi_0 | . \tag{3.16}$$

Since $b_0 = 1$, the above equation reduces to

$$| \xi_k | \quad \leq \quad | \xi_0 | . \tag{3.17}$$

Hence, the assertion is valid for $n = k$. Therefore, (3.11) is valid for every n. i.e.

$$| \xi_n | \quad \leq \quad | \xi_0 | . \tag{3.18}$$

By means of (3.5) and (3.18) we have

$$\| \zeta^n \|_2 = \left(\sum_{m=1}^{M-1} h | \zeta_m^n |^2 \right)^{\frac{1}{2}} = \left(\sum_{-\infty}^{\infty} | \zeta_n(l) |^2 \right)^{\frac{1}{2}} = \| \zeta^0 \|_2 . \tag{3.19}$$

Hence, we conclude that

$$\| \zeta^n \|_2 \quad \leq \quad \| \zeta^0 \|_2 . \tag{3.20}$$

Therefore, the present numerical scheme (2.21)-(2.23) for solving (2.1)-(2.3) is unconditionally stable.

3.2 Stability Analysis of numerical scheme of method (2.51)-(2.53)

In this section, we establish stability analysis of the proposed method (2.51)-(2.53) for solving (2.24)-(2.26). Let V_m^n be the approximate solution of v_m^n. Define the error ζ_m^n as

$$\zeta_m^n = v_m^n - V_m^n \tag{3.21}$$

By (3.21), we obtain the round-off error expression as follows:

$$
\begin{aligned}
&\zeta_{m-1}^{n}\Bigg(-\frac{1}{h^2}+\frac{2(P_1')_m+R_m-(P_1)_m^2}{12}-\frac{(P_1)_m}{2h}\\
&\quad -\frac{h((P_1)_m''-(P_1)_m(P_1')_m-(P_1)_mR_m+2(P_2')_m)}{24}\\
&\quad +\frac{((s_n-s_{n-1})^{-\alpha})(2+(P_1)_mh)}{24\Gamma(2-\alpha)}\Bigg)\\
&+\zeta_{m}^{n}\Bigg(\frac{2}{h^2}-\frac{2(P_1')_m+R_m-(P_1)_m^2}{6}+(P_2)_m\\
&\quad +\frac{h^2(R_m''-(P_1)_mR_m)}{12}+\frac{5((s_n-s_{n-1})^{-\alpha})}{6\Gamma(2-\alpha)}\Bigg)\\
&+\zeta_{m+1}^{n}\Bigg(-\frac{1}{h^2}+\frac{2(P_1')_m+R_m-(P_1)_m^2}{12}+\frac{(P_1)_m}{2h}\\
&\quad +\frac{h((P_1)_m''-(P_1)_m(P_1')_m-(P_1)_mR_m+2(P_2')_m)}{24}\\
&\quad +\frac{((s_n-s_{n-1})^{-\alpha})(2-(P_1)_mh)}{24\Gamma(2-\alpha)}\Bigg)\\
&=\frac{1}{\Gamma(2-\alpha)}\sum_{j=0}^{n-2}\frac{(s_n-s_j)^{1-\alpha}-(s_n-s_{j+1})^{1-\alpha}}{s_{j+1}-s_j}\\
&\quad \times\Bigg((\zeta_{m-1}^{j+1}-\zeta_{m-1}^{j})\left(\frac{-2-(P_1)_mh}{24}\right)+(\zeta_{m}^{j+1}-\zeta_{m}^{j})\left(-\frac{5}{6}\right)\\
&\quad +(\zeta_{m+1}^{j+1}-\zeta_{m+1}^{j})\left(\frac{-2+(P_1)_mh}{24}\right)\Bigg)\\
&\quad -\frac{(s_n-s_{n-1})^{-\alpha}}{\Gamma(2-\alpha)}\Bigg(\zeta_{m-1}^{n-1}\left(\frac{-2-(P_1)_mh}{24}\right)\\
&\quad +\zeta_{m}^{n-1}\left(-\frac{5}{6}\right)+\zeta_{m+1}^{n-1}\left(\frac{-2+(P_1)_mh}{24}\right)\Bigg).
\end{aligned}
\tag{3.22}
$$

The RHS of above equation can be re-written as:

$$
\begin{aligned}
RHS = \frac{1}{\Gamma(2-\alpha)} \Bigg[& - \left(\frac{(s_n - s_0)^{1-\alpha} - (s_n - s_1)^{1-\alpha}}{s_1 - s_0} \right) \\
& \times \left\{ \zeta_{m-1}^{0} \left(\frac{-2 - (P_1)_m h}{24} \right) + \zeta_m^0 \left(-\frac{5}{6} \right) + \zeta_{m+1}^0 \left(\frac{-2 + (P_1)_m h}{24} \right) \right\} \\
& - \sum_{j=1}^{n-1} \left(\frac{(s_n - s_{n-j})^{1-\alpha} - (s_n - s_{n-j+1})^{1-\alpha}}{s_{n-j+1} - s_{n-j}} - \frac{(s_n - s_{n-j-1})^{1-\alpha} - (s_n - s_{n-j})^{1-\alpha}}{s_{n-j} - s_{n-j-1}} \right) \\
& \times \Bigg((\zeta_{m-1}^{n-j+1} - \zeta_{m-1}^{n-j}) \left(\frac{-2 - (P_1)_m h}{24} \right) + (\zeta_m^{n-j+1} - \zeta_m^{n-j}) \left(-\frac{5}{6} \right) \\
& + (\zeta_{m+1}^{n-j+1} - \zeta_{m+1}^{n-j}) \left(\frac{-2 + (P_1)_m h}{24} \right) \Bigg) \Bigg].
\end{aligned}
\tag{3.23}
$$

Define a grid function $\zeta^n(y)$ for $n = 1, 2, 3, ..., N$ as

$$
\zeta^n(y) = \begin{cases} \zeta_m^n, & \text{if} \quad y \in (y_{m-\frac{1}{2}}, y_{m+\frac{1}{2}}], m = 1, 2, ..., M-1, \\ 0, & \text{if} \quad y \in [0, \frac{h}{2}] \cup (1 - \frac{h}{2}, 1] \end{cases}
\tag{3.24}
$$

and let $\zeta^n = [\zeta_1^n, \zeta_2^n, ..., \zeta_{M-1}^n]^T$. Define the following norm

$$
\| \zeta^n \|_2 = \left(\sum_{m=1}^{M-1} h \mid \zeta_m^n \mid^2 \right)^{\frac{1}{2}} = \left(\sum_{-\infty}^{\infty} \mid \zeta_n(l) \mid^2 \right)^{\frac{1}{2}}, n = 0, 1, 2, ..., N,
\tag{3.25}
$$

where $\zeta_n(l)$ is the Fourier coefficient (FC) of the series for $\zeta^n(y)$. We write ζ_m^n in the following form

$$
\zeta_m^n = \xi_n e^{\iota m \rho h},
\tag{3.26}
$$

where $\iota = \sqrt{-1}$. Inserting (3.26) in (3.22) and (3.23) gives

$$\begin{aligned}
&\xi_n\Bigg[\left(-\frac{1}{h^2}+\frac{2(P_1')_m+R_m-(P_1^2)_m}{12}+\frac{1}{\Gamma(2-\alpha)(s_n-s_{n-1})^\alpha}\right)(2\cos\rho h)\\
&\quad+\left(\frac{(P_1)_m}{2h}+\frac{h((P_1'')_m-(P_1)_m(P_1')_m-(P_1)_mR_m+2(P_2')_m)}{24}-\frac{(P_1)_mh}{24\Gamma(2-\alpha)(s_n-s_{n-1})^\alpha}\right)\\
&\quad(2\iota\sin\rho h)\\
&\quad+\frac{2}{h^2}-\frac{2(P_1')_m+R_m-(P_1^2)_m}{6}+(P_2)_m+\frac{h^2(R_m''-(P_1)_mR_m)}{12}+\frac{5}{6\Gamma(2-\alpha)(s_n-s_{n-1})^\alpha}\Bigg]\\
&=\frac{1}{\Gamma(2-\alpha)}\left[e^{-\iota\rho h}\left(\frac{-2-(P_1)_mh}{24}\right)+\left(-\frac{5}{6}\right)+e^{\iota\rho h}\left(\frac{-2+(P_1)_mh}{24}\right)\right]\\
&\quad\times\Bigg[-\left(\frac{(s_n-s_0)^{1-\alpha}-(s_n-s_1)^{1-\alpha}}{s_1-s_0}\right)\xi_0\\
&\quad-\sum_{j=1}^{n-1}\left(\frac{(s_n-s_{n-j})^{1-\alpha}-(s_n-s_{n-j+1})^{1-\alpha}}{s_{n-j+1}-s_{n-j}}-\frac{(s_n-s_{n-j-1})^{1-\alpha}-(s_n-s_{n-j})^{1-\alpha}}{s_{n-j}-s_{n-j-1}}\right)\\
&\quad(\xi_{n-j+1}-\xi_{n-j})\Bigg].
\end{aligned}\tag{3.27}$$

Consider

$$a_{n,k}:=\frac{(s_n-s_{n-k})^{(1-\alpha)}-(s_n-s_{n-k+1})^{(1-\alpha)}}{(\Gamma(2-\alpha))(s_{n-k+1}-s_{n-k})}$$

and

$$a_{n,1}:=\frac{1}{\Gamma(2-\alpha)(s_n-s_{n-1})^\alpha}.$$

Multiplying equation (3.27) by $\frac{1}{a_{n,1}}$ then solving for ξ_n, we get:

$$\xi_n=\frac{\frac{A}{a_{n,1}}\Big(-a_{n,n}\xi_0-\sum_{j=1}^{n-1}(a_{n-j}-a_{n-j+1})(\xi_{n-j+1}-\xi_{n-j})\Big)}{\frac{1}{a_{n,1}}\Big(B(2cos\rho h)+C(2\iota sin\rho h)+D\Big)},n\geqslant 1.\tag{3.28}$$

where

$$A:=\left(e^{-\iota\rho h}(\frac{-2-(P_1)_mh}{24})-\frac{5}{6}+e^{\iota\rho h}(\frac{-2+(P_1)_mh}{24})\right),$$

$$B := \bigg(-\frac{1}{h^2} + \frac{2(P_1')_m + R_m - (P_1^2)_m}{12} + a_{n,1} \bigg),$$

$$C := \frac{h((P_1")_m - (P_1)_m(P_1')_m - (P_1)_m R_m + 2(P_2')_m)}{24} - \frac{a_{n,1}(P_1)_m h}{24} \bigg),$$

$$D := \frac{2}{h^2} - \frac{2(P_1')_m + R_m - (P_1^2)_m}{6} + (P_2)_m + \frac{h^2(R_m" - (P_1)_m R_m)}{12} \frac{5a_{n,1}}{6}.$$

Lemma 1. For sufficiently small h ,the following inequality hold true:

$$\frac{A}{\frac{1}{a_{n,1}}(B(2cos\rho h) + C(2\iota sin\rho h) + D)} \leqslant 1, \forall n \geqslant 1. \tag{3.29}$$

Lemma 2. Suppose that $\xi_n (n = 1, 2, ..., N)$ are the solution of (3.29),then

$$|\xi_n| \leq |\xi_0|, \quad n = 1, 2, ..., N. \tag{3.30}$$

Proof. We use mathematical induction principle to prove this result. For $n = 1$, equation (3.28) leads to

$$\xi_1 = \frac{\frac{A}{a_{1,1}} \bigg(- a_{1,1} \bigg)}{\frac{1}{a_{1,1}} \bigg(B(2cos\rho h) + C(2\iota sin\rho h) + D \bigg)} \xi_0. \tag{3.31}$$

From Lemma 1 and equation (3.31), it follows that

$$|\xi_1| \leqslant |\xi_0|.$$

Now, assume that

$$|\xi_n| \leqslant |\xi_0|, \quad n = 1, 2, ..., p-1. \tag{3.32}$$

Setting $n = p$ in equation(3.28) and using equation (3.32), we obtain

$$|\xi_p| \leq \frac{|\frac{A}{a_{p,1}}|}{|\frac{1}{a_{p,1}}||B(2cos\rho h) + C(2\iota sin\rho h) + D|} |\xi_0|. \tag{3.33}$$

Finally, making use of Lemma 1, from (3.33), we get

$$|\xi_p| \leqslant |\xi_0|.$$

This proves Lemma 2.

Theorem 1. The compact FDM given by (2.51) for solving the model problem (2.24)-(2.26) is unconditionally stable.

Proof. By means of (3.25) and (3.30), we have

$$\| \zeta^n \|_2 = \left(\sum_{m=1}^{M-1} h \mid \zeta_m^n \mid^2 \right)^{\frac{1}{2}} = \left(\sum_{-\infty}^{\infty} \mid \zeta_n(k) \mid^2 \right)^{\frac{1}{2}} = \| \zeta^0 \|_2 \, . \tag{3.34}$$

Hence, we conclude that

$$\| \zeta^n \|_2 \quad \leq \quad \| \zeta^0 \|_2, \quad n = 1, 2, ..., N. \tag{3.35}$$

Therefore, the present numerical scheme (2.51) for solving (2.24)-(2.26) is unconditionally stable.

Chapter 4

Convergence Analysis

In this chapter, we provide convergence result of the proposed methods.

4.1 Convergence analysis of method (2.21)-(2.23)

Here, we analyze the convergence of the proposed numerical scheme defined by (2.21)-(2.23).

Substracting equation (2.21) from (2.19), we get the error equation

$$\begin{aligned}
&\left(\frac{-t}{h^2}-\frac{e_m^{n-1}}{2h}\right)e_{m-1}^n+\left(\frac{2v}{h^2}+\frac{e_{m+1}^{n-1}-e_{m-1}^{n-1}}{2h}+w\right)e_m^n\\
&+\left(\frac{-v}{h^2}+\frac{e_m^{n-1}}{2h}\right)e_{m+1}^n=-\frac{e_m^{n-1}e_{m-1}^{n-1}-e_m^{n-1}e_{m+1}^{n-1}}{2h}\\
&\quad+w\left(\sum_{j=1}^{n-1}e_m^{n-j}(b_{j-1}-b_j)\right)+\mathcal{R}_m^n,\quad m=1,2,3,...,M-1,\quad n=1,2,3,...,N,
\end{aligned}\tag{4.1}$$

where

$$e_m^n=u_m^n-U_m^n,\quad w=\frac{(s_n-s_{n-1})^{-\alpha}}{\Gamma(2-\alpha)}.\tag{4.2}$$

with

$$e_0^n=e_M^n=0,\quad e_m^0=0,\quad m=1,2,3,...,M-1,n=1,2,3,...,N\tag{4.3}$$

Now, introduce the following grid functions:

$$e^n(y) = \begin{cases} e_m^n, & \text{if} \quad y \in (y_{m-\frac{1}{2}}, y_{m+\frac{1}{2}}], m = 1, 2, ..., M-1, \\ 0, & \text{if} \quad y \in [0, \frac{h}{2}] \cup (1 - \frac{h}{2}, 1]. \end{cases} \tag{4.4}$$

$$\mathcal{R}^n(y) = \begin{cases} \mathcal{R}_m^n, & \text{if} \quad y \in (y_{m-\frac{1}{2}}, y_{m+\frac{1}{2}}], m = 1, 2, ..., M-1, \\ 0, & \text{if} \quad y \in [0, \frac{h}{2}] \cup (1 - \frac{h}{2}, 1]. \end{cases} \tag{4.5}$$

and, let $e^n = [e_1^n, e_2^n, ..., e_{M-1}^n]^T$, $\mathcal{R}^n = [\mathcal{R}_1^n, \mathcal{R}_2^n, ..., \mathcal{R}_{M-1}^n]^T$. Also, we define the following norms

$$||e^n||_2 = \left(\sum_{m=1}^{M-1} h|e_m^n|^2 \right)^{1/2} = \left(\sum_{l=-\infty}^{\infty} |\mu_n(l)|^2 \right)^{1/2}, n = 0, 1, ..., N, \tag{4.6}$$

and

$$||\mathcal{R}^n||_2 = \left(\sum_{m=1}^{M-1} h|\mathcal{R}_m^n|^2 \right)^{1/2} = \left(\sum_{l=-\infty}^{\infty} |\sigma_n(l)|^2 \right)^{1/2}, n = 0, 1, ..., N, \tag{4.7}$$

where $\mu_n(l)$ and $\sigma_n(l)$ respectively represents the Fourier coefficients of the series for $e^n(y)$ and $\mathcal{R}^n(y)$. Suppose that $\mathcal{R}_m^n$ and e_m^n have the following forms

$$e_m^n = \mu_n e^{\iota m \rho h}, \quad \mathcal{R}_m^n = \sigma_n e^{\iota m \rho h}. \tag{4.8}$$

Substituting equation (4.8) into equation (4.1), we have

$$\begin{aligned} &\mu_n \left[\left(-\frac{2t \cos \rho h}{h^2} \frac{2t}{h^2} + w \right) + \iota \left(\frac{\sin \rho h (2\mu_{n-1} e^{\iota m \rho h})}{h} \right) \right] \\ &= \left[\frac{\iota \mu_{n-1}(e^{\iota m \rho h}) \sin \rho h}{h} + w \left(\sum_{j=1}^{n-1} \mu_{n-j}(b_{j-1} - b_j) \right) \right] + \sigma_n. \end{aligned} \tag{4.9}$$

Equation (4.9) implies that

$$\mu_n = \frac{\frac{\iota\mu_{n-1}(e^{\iota m\rho h})\sin\rho h}{h} + w\left(\sum_{j=1}^{n-1}\mu_{n-j}(b_{j-1}-b_j)\right)}{\frac{4t\sin^2(\frac{\rho h}{2})}{h^2} + w + \iota\left(\frac{2\mu_{n-1}e^{\iota m\rho h}\sin\rho h}{h}\right)} + \frac{\sigma_n}{\frac{4t\sin^2(\frac{\rho h}{2})}{h^2} + w + \iota\left(\frac{2\mu_{n-1}e^{\iota m\rho h}\sin\rho h}{h}\right)}. \tag{4.10}$$

Since $\Delta s > 0$, $h > 0$ and $0 < \alpha < 1$. So, $\Gamma(2-\alpha) > 0$ and $t > 1$. Thus, we can write

$$\frac{1}{\left(\frac{4t\sin^2\frac{\rho h}{2}}{h^2} + w\right)} \leqslant \frac{1}{\left(\frac{4t}{h^2} + w\right)} \leqslant 1. \tag{4.11}$$

From equation (2.20), there is a positive constant $\mathcal{C}$ such that

$$|\mathcal{R}_m^n| \quad \leqslant \mathcal{C}(h^2 + (\Delta s)^{-min\{2-\alpha, r\alpha\}}), m = 1, 2, ..., M-1, n = 1, 2, ..., N. \tag{4.12}$$

From equation (4.7), we can obtain

$$\begin{aligned} ||\mathcal{R}^n||_2 &\leqslant \left(\sum_{m=1}^{M-1} h(\mathcal{C}(h^2 + \Delta s^{-min\{2-\alpha, r\alpha\}}))^2\right)^{1/2} \\ &\leqslant \sqrt{Mh}(\mathcal{C}(h^2 + \Delta s^{-min\{2-\alpha, r\alpha\}})) = \mathcal{D}_1(h^2 + \Delta s^{-min\{2-\alpha, r\alpha\}}). \end{aligned} \tag{4.13}$$

By the means of equation (4.13), the series in the right side of (4.7), (i.e.$(\sum_{l=-\infty}^{\infty}|\sigma_n(l)|^2)^{1/2}$) converges. Then, there is a positive constant $\mathcal{D}_2$ such that

$$|\sigma_n| \equiv |\sigma_n(l)| \leqslant \mathcal{D}_2\Delta s|\sigma_1| \equiv \mathcal{D}_2\Delta s|\sigma_1(l)|, \quad n = 1, 2..., N. \tag{4.14}$$

Theorem The proposed numerical scheme (2.21) is L_2-convergent with convergence order

$$||e^n||_2 = \mathcal{O}((\Delta s)^{-min\{2-\alpha, r\alpha\}} + h^2). \tag{4.15}$$

Proof We first prove the following results by means of mathematical induction.

$$|\mu_n| \leqslant \mathcal{D}_2(1 + \Delta s)^n|\sigma_1|, \quad n = 1, 2, ..., N. \tag{4.16}$$

Considering $n = 1$ in equation (4.10) and then applying (4.11) produces

$$|\mu_1| \leqslant \frac{|\sigma_1|}{(\frac{4t\sin^2(\frac{\rho h}{2})}{h^2} + w) + \iota(\frac{2\mu_{n-1}e^{\iota m\rho h}\sin\rho h}{h})} \leqslant |\sigma_1| \leqslant \mathcal{D}_2(1+\Delta s)|\sigma_1|. \tag{4.17}$$

Therefore, (4.16) is valid for $n = 1$. Now, we assume that (4.16) is valid for $n \leqslant j-1$, i.e.,

$$|\mu_n| \leqslant \mathcal{D}_2(1+\Delta s)^n|\sigma_1|, \quad n = 1, 2, ..., j-1. \tag{4.18}$$

For $n = j$, (4.10) leads to

$$\begin{aligned} |\mu_j| \leqslant & \frac{\left[\frac{\iota\mu_{j-1}(e^{\iota m\rho h})\sin\rho h}{h} + w\left(\sum_{k=1}^{j-1}\mu_{j-k}(b_{k-1}-b_k)\right)\right]}{(\frac{4t\sin^2(\frac{\rho h}{2})}{h^2} + w) + \iota(\frac{2\mu_{j-1}e^{\iota m\rho h}\sin\rho h}{h})} \\ & + \frac{|\sigma_j|}{(\frac{4t\sin^2(\frac{\rho h}{2})}{h^2} + w) + \iota(\frac{2\mu_{j-1}e^{\iota m\rho h}\sin\rho h}{h})}. \end{aligned} \tag{4.19}$$

By using (4.11) into (4.19), we obtain

$$|\mu_j| \leqslant \sum_{k=1}^{j-1}(b_{k-1}-b_k)|\mu_{j-k}| + |\sigma_j|. \tag{4.20}$$

Now, using (4.18) and (4.14) in (4.20), we obtain

$$\begin{aligned} |\mu_j| &\leqslant \sum_{k=1}^{j-1}(b_{k-1}-b_k)\mathcal{D}_2(1+\Delta s)^{j-k}|\sigma_1| + \mathcal{D}_2\Delta s|\sigma_1| \\ &\leqslant \mathcal{D}_2(1+\Delta s)^{i-1}(1-b_{j-1})|\sigma_1| + (1+\Delta s)\mathcal{D}_2|\sigma_1| \\ &\leqslant \mathcal{D}_2(1+\Delta s)^j|\sigma_1|. \end{aligned} \tag{4.21}$$

Thus, (4.16) is valid for $n = j$. As a result, the assertion (4.16) is valid $\forall \quad n \geqslant 1$.

Taking into the account (4.6), (4.7), (4.13) and (4.16), we have

$$\begin{aligned}||e^n||_2 \leqslant \Big(\sum_{k=-\infty}^{\infty} (\mathcal{D}_2^2(1+\Delta s)^{2n}|\sigma_1(k)|^2\Big)^{1/2} &= \mathcal{D}_2(1+\Delta s)^n(\sum_{l=-\infty}^{\infty} |\sigma_1(l)|^2)^{1/2} \\ = \mathcal{D}_2(1+\Delta s)^n||\mathcal{R}^1||_2 &\leqslant \mathcal{D}_1\mathcal{D}_2(1+\Delta s)^n(h^2+(\Delta s)^{-min\{2-\alpha,r\alpha\}}) \\ &\leqslant \mathcal{D}_1\mathcal{D}_2 exp(n\Delta s)(h^2+(\Delta s)^{-min\{2-\alpha,r\alpha\}}).\end{aligned} \tag{4.22}$$

Since, $n\Delta s \leqslant S$, it follows from (4.22) that

$$||e^n||_2 \leqslant \mathcal{D}(\Delta s^{-min\{2-\alpha,r\alpha\}} + h^2), \quad \mathcal{D} = \mathcal{D}_1\mathcal{D}_2 exp(S). \tag{4.23}$$

Hence, proof of the theorem is completed.

4.2 Convergence analysis of the method (2.51)-(2.53)

Here, we analyze the convergence of the proposed numerical scheme (2.51). Substracting equation (2.51) from (2.48), we get the error equation

$$\begin{aligned}
&e_{m-1}^n\Bigg(-\frac{1}{h^2} + \frac{2(P_1')_m + R_m - (P_1)_m^2}{12} - \frac{(P_1)_m}{2h} \\
&- \frac{h((P_1)_m'' - (P_1)_m(P_1')_m - (P_1)_m R_m + 2(P_2')_m)}{24} + \frac{((s_n - s_{n-1})^{-\alpha})(2+(P_1)_m h)}{24\Gamma(2-\alpha)}\Bigg) \\
&+ e_m^n\Bigg(\frac{2}{h^2} - \frac{2(P_1')_m + R_m - (P_1)_m^2}{6} + (P_2)_m + \frac{h^2(R_m'' - (P_1)_m R_m)}{12} + \frac{5((s_n - s_{n-1})^{-\alpha})}{6\Gamma(2-\alpha)}\Bigg) \\
&+ e_{m+1}^n\Bigg(-\frac{1}{h^2} + \frac{2(P_1')_m + R_m - (P_1)_m^2}{12} + \frac{(P_1)_m}{2h} \\
&+ \frac{h((P_1)_m'' - (P_1)_m(P_1')_m - (P_1)_m R_m + 2(P_2')_m)}{24} + \frac{((s_n - s_{n-1})^{-\alpha})(2-(P_1)_m h)}{24\Gamma(2-\alpha)}\Bigg) \\
&= \frac{1}{\Gamma(2-\alpha)} \sum_{j=0}^{n-2} \frac{(s_n - s_j)^{1-\alpha} - (s_n - s_{j+1})^{1-\alpha})}{s_{j+1} - s_j} \\
&\Bigg((e_{m-1}^{j+1} - e_{m-1}^j)(\frac{-2-(P_1)_m h}{24}) + (e_m^{j+1} - e_m^j)(-5/6) + (e_{m+1}^{j+1} - e_{m+1}^j)((-2+(P_1)_m h)/24)\Bigg) \\
&- \frac{(s_n - s_{n-1})^{-\alpha}}{\Gamma(2-\alpha)}\Bigg(e_{m-1}^{n-1}((-2-(P_1)_m h)/24) + e_m^{n-1}(-5/6) + e_{m+1}^{n-1}((-2+(P_1)_m h)/24)\Bigg).
\end{aligned} \tag{4.24}$$

where,

$$e_m^n = u_m^n - v_m^n. \tag{4.25}$$

with

$$e_0^n = e_M^n = 0, \quad e_m^0 = 0, \quad m = 1, 2, 3, ..., M-1, n = 1, 2, 3, ..., N \tag{4.26}$$

Now, introduce the following grid functions:

$$e^n(y) = \begin{cases} e_m^n, & \text{if} \quad y \in (y_{m-\frac{1}{2}}, y_{m+\frac{1}{2}}], m = 1, 2, ..., M-1, \\ 0, & \text{if} \quad y \in [0, \frac{h}{2}] \cup (1 - \frac{h}{2}, 1]. \end{cases} \tag{4.27}$$

$$\mathcal{R}^n(y) = \begin{cases} \mathcal{R}_m^n, & \text{if} \quad y \in (y_{m-\frac{1}{2}}, y_{m+\frac{1}{2}}], m = 1, 2, ..., M-1, \\ 0, & \text{if} \quad y \in [0, \frac{h}{2}] \cup (1 - \frac{h}{2}, 1]. \end{cases} \tag{4.28}$$

and let $e^n = [e_1^n, e_2^n, ..., e_{M-1}^n]^T$, $\mathcal{R}^n = [\mathcal{R}_1^n, \mathcal{R}_2^n, ..., \mathcal{R}_{M-1}^n]^T$. Also, we define the following norms

$$||e^n||_2 = \left(\sum_{m=1}^{M-1} h|e_m^n|^2 \right)^{1/2} = \left(\sum_{l=-\infty}^{\infty} |\mu_n(l)|^2 \right)^{1/2}, n = 0, 1, ..., N \tag{4.29}$$

and

$$||\mathcal{R}^n||_2 = \left(\sum_{m=1}^{M-1} h|\mathcal{R}_m^n|^2 \right)^{1/2} = \left(\sum_{l=-\infty}^{\infty} |\sigma_n(l)|^2 \right)^{1/2}, n = 0, 1, ..., N \tag{4.30}$$

where $\mu_n(l)$ and $\sigma_n(l)$ respectively represents the Fourier coefficients of the series for $e^n(y)$ and $\mathcal{R}^n(y)$. Suppose that $\mathcal{R}_m^n$ and e_m^n have the following forms

$$e_m^n = \mu_n e^{\iota m \rho h}, \quad \mathcal{R}_m^n = \sigma_n e^{\iota m \rho h}. \tag{4.31}$$

Substituting equation (4.31) into equation (4.24), after simplification, we obtain

the following expression :

$$\mu_n = \frac{\frac{A}{a_{n,1}}\Big(- a_{n,n}\xi_0 - \sum_{j=1}^{n-1}(a_{n-j} - a_{n-j+1})(\xi_{n-j+1} - \xi_{n-j})\Big) + \sigma_n}{\frac{1}{a_{n,1}}\Big(B(2cos\rho h) + C(2\iota sin\rho h) + D\Big)}, n \geqslant 1. \quad (4.32)$$

From equation (2.50), there is a positive constant $\mathcal{C}$ such that

$$|\mathcal{R}_m^n| \quad \leqslant \mathcal{C}(h^4 + (\Delta s)^{2-\alpha}), m = 1, 2, ..., M-1, n = 1, 2, ..., N. \quad (4.33)$$

From equation (4.30), we can obtain

$$\begin{aligned} ||\mathcal{R}^n||_2 &\leqslant \Big(\sum_{m=1}^{M-1} h(\mathcal{C}(h^4 + \Delta s^{2-\alpha}))^2\Big)^{1/2} \\ &\leqslant \sqrt{Mh}(\mathcal{C}(h^4 + \Delta s^{2-\alpha})) = \mathcal{D}_1(h^4 + \Delta s^{2-\alpha}). \end{aligned} \quad (4.34)$$

By means of equation (4.34), the series in the right side of (4.30), (i.e.$(\sum_{l=-\infty}^{\infty} |\sigma_n(l)|^2)^{1/2}$) converges. Then there is a positive constant $\mathcal{D}_2$ such that

$$|\sigma_n| \equiv |\sigma_n(l)| \leqslant \mathcal{D}_2\Delta s|\sigma_1| \equiv \mathcal{D}_2\Delta s|\sigma_1(l)|, \quad n = 1, 2..., N. \quad (4.35)$$

Lemma 3. For $n = 1, 2, ..., N.$, we have

$$|\mu_n| \leqslant \mathcal{D}_2(1 + \Delta s)^n|\sigma_1|, \quad (4.36)$$

where $\mathcal{D}_2$ is the constant in (4.35).

Proof. We use mathematical induction principle to prove this result. For $n = 1$, equation (4.32) yields

$$\mu_1 = \frac{\sigma_1}{\frac{1}{a_{1,1}}\Big(B(2cos\rho h) + C(2\iota sin\rho h) + D\Big)}. \quad (4.37)$$

Making use of (4.35), we obtain

$$|\mu_1| \leq |\sigma_1| \leqslant \mathcal{D}_2(1+\Delta s)^n|\sigma_1|. \tag{4.38}$$

Now, assume that

$$|\mu_n| \leqslant \mathcal{D}_2(1+\Delta s)^n|\sigma_1|, \quad n = 1, 2, ..., p-1. \tag{4.39}$$

Setting $n = p$ in equation (4.32), we get

$$|\mu_p| \leqslant \left| \sum_{j=1}^{p-1} (a_{p-j} - a_{p-j+1})(\mu_{p-j+1} - \mu_{p-j}) \right| + |\sigma_p|. \tag{4.40}$$

Using equations (4.35) and (4.39) in equation (4.40), we get

$$\begin{aligned} |\mu_p| &\leqslant \sum_{j=1}^{p-1} (a_{p-j} - a_{p-j+1})(\mathcal{D}_2(1+\Delta s)^{p-j+1} - \mathcal{D}_2(1+\Delta s)^{p-j})|\sigma_1| + \mathcal{D}_2\Delta s|\sigma_1| \\ &\leqslant \mathcal{D}_2(1+\Delta s)^p|\sigma_1|. \end{aligned} \tag{4.41}$$

which proves lemma 3.

Theorem 2. The present compact FDM (2.51) is L_2-convergent with

$$||e^n||_2 = \mathcal{O}((\Delta s)^{2-\alpha} + h^4). \tag{4.42}$$

Proof. Taking into the account (4.29),(4.30),(4.34) and(4.36), we have

$$\begin{aligned} ||e^n||_2 \leqslant \left(\sum_{l=-\infty}^{\infty} (\mathcal{D}_2^2(1+\Delta s)^{2n}|\sigma_1(l)|^2 \right)^{1/2} &= \mathcal{D}_2(1+\Delta s)^n(\sum_{l=-\infty}^{\infty} |\sigma_1(l)|^2)^{1/2} \\ = \mathcal{D}_2(1+\Delta s)^n||\mathcal{R}^1||_2 \leqslant \mathcal{D}_1\mathcal{D}_2(1+\Delta s)^n(h^4 + (\Delta s)^{2-\alpha}) \\ \leqslant \mathcal{D}_1\mathcal{D}_2 exp(n\Delta s)(h^4 + (\Delta s)^{2-\alpha}). \end{aligned} \tag{4.43}$$

Since, $n\Delta s \leqslant S$, it follows from (4.43) that

$$||e^n||_2 \leqslant \mathcal{D}(\Delta s^{2-\alpha} + h^4), \quad \mathcal{D} = \mathcal{D}_1\mathcal{D}_2 exp(S). \tag{4.44}$$

Hence, proof of the theorem is completed.

Chapter 5

Numerical Results

This chapter provides numerical examples designed to validate the theoretical findings presented earlier.

For all numerical experiments, we have used MATLAB $R2024b$ on a computer with an 12th Gen Intel(R) Core(TM) $i5-1235U$ 1.30GHz processor.

5.1 Numerical Illustration for TFBE

We evaluate the L_∞ errors (E1) in order to check the accuracy of numerical result obtained by the developed algorithm. The errors are computed by using the following equation:

$$E_1 = \max_{1\leq n\leq N}\max_{1\leq m\leq M}\left|U_m^n - u_m^n\right|. \tag{5.1}$$

The rate of convergence in space and time direction are calculated by:

$$ROC(in\ space) = \frac{log\left(\frac{E_1(2h,\tau_n)}{E_1(h,\tau_n)}\right)}{log(2)}. \tag{5.2}$$

$$ROC(in\ time) = \frac{log\left(\frac{E_1(h,2\tau_n)}{E_1(h,\tau_n)}\right)}{log(2)}. \tag{5.3}$$

Example 5.1.1 Consider the TFBE (2.1)-(2.3) with $t = 1, Y_l = 0, Y_r = 1, f(y) = 0, \theta_1 = 0, \theta_2 = t^\alpha sin(1)$ and $L(y,s) = sin(y)(\Gamma(1+\alpha) + t^{2\alpha}cos(y) + ts^\alpha)$.

The exact solution is $u(y,s) = s^{\alpha}\sin(y)$, which is a non-smooth function. We apply the developed method to solve this problem. Table (5.1) provides the L_∞ errors and their corresponding ROCs in time direction on the graded mesh for $\alpha = 0.5, 0.7$. Table (5.2) provides the L_∞ errors in uniform mesh and the corresponding ROC for $\alpha = 0.5, 0.7$. In table (5.3), we compute the maximum absolute errors and their corresponding ROCs in space direction by fixing $N = 10000$.

Table 5.1: L_∞ norm errors for example 5.2.1 when $M = 256$ and $r = \frac{2-\alpha}{\alpha}$

α	N	L_∞ errors	order(d)
	256	$7.7904e-05$	
0.5	512	$2.9888e-05$	1.3821
	1024	$1.2112e-05$	1.4145
	2048	$4.1419e-06$	1.4367
	256	$1.6772e-04$	
0.7	512	$7.5975e-05$	1.1425
	1024	$3.3618e-05$	1.1763
	2048	$1.4609e-05$	1.2024

Figure 5.1: 3D graph of numerical solution of example 5.1.1 with $M = N = 64$

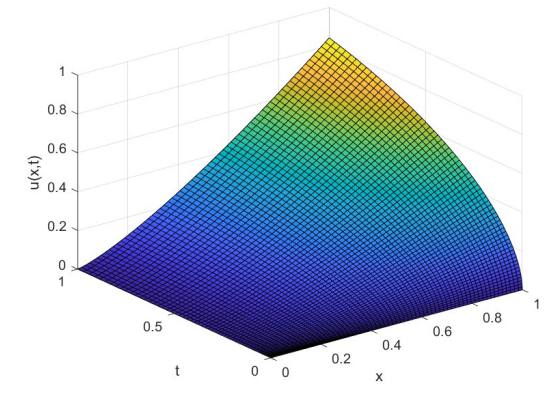

Table 5.2: L_∞ norm errors for example 5.1.1 when $M = 256$ and $r = 1$

α	N	L_∞ errors	order(d)
	256	0.0052	
0.5	512	0.0042	0.3081
	1024	0.0033	0.3471
	2048	0.0025	0.4005
	256	0.0021	
0.7	512	0.0014	0.5850
	1024	$9.1952e-04$	0.6065
	2048	$5.9869e-04$	0.6191

Table 5.3: L_∞ norm errors for example 5.1.1 when $N = 10000$

α	M	L_∞ errors	order(d)
	4	$6.8435e-04$	
0.5	8	$1.7493e-04$	1.9680
	16	$4.3932e-05$	1.9934
	4	$6.7362e-04$	
0.7	8	$1.7235e-04$	1.9666
	16	$4.3242e-05$	1.9948

Figure 5.2: 3D graph of exact solution of example 5.1.1 with $M = N = 64$

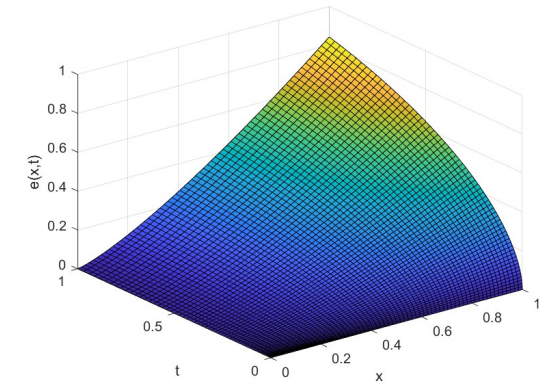

Figure 5.3: 3D graph of error of example 5.1.1

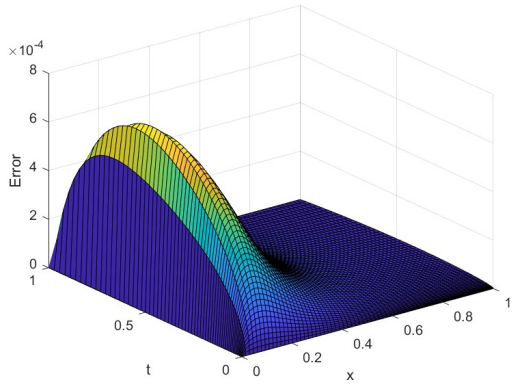

5.2 Numerical Illustration for TFFPE

Example 5.2.1 Consider the TFFPE (2.24)-(2.26) with $Y_l = 0$, $Y_r = 1$, $f(y) = 0$, $\theta_1 = 0$, $\theta_2 = s^\alpha sin(\pi)$,$P(y) = -exp(y-0.5)^2$ and $L(y) = \alpha\Gamma(\alpha)\sin(\pi y) - t^\alpha exp(y - 0.5)^2[2(y-0.5)\sin(\pi y) + \pi\cos(\pi y)] + \pi^2 t^\alpha \sin(\pi y))$.

The exact solution for this problem is $u = s^\alpha \sin(\pi y)$. Table (5.4) presents the L_∞ errors and their corresponding rate of convergence (ROC) in temporal direction when $M = 256$, while table (5.5) presents the L_∞ errors and their corresponding rate of convergence (ROC) in spatial direction when $N = 5000$.

Table 5.4: L_∞ norm errors for example 5.2.1 when $M = 256$ and $r = \frac{2-\alpha}{\alpha}$

α	N	L_∞ errors	order(d)	CPU time(s)
	256	$4.4840e-05$		1.8869
0.3	512	$1.4759e-05$	1.6032	6.940
	1024	$4.8065e-06$	1.6185	27.439
	2048	$1.5513e-06$	1.6315	108.068
	256	$7.0256e-05$		1.950
0.4	512	$2.4328e-05$	1.5300	6.814
	1024	$8.3327e-06$	1.5458	27.124
	2048	$2.8341e-06$	1.5559	119.801

Figures (5.4) and (5.6) show the surface plots of approximate and exact solutions, when $M = N = 50$ and $\alpha = 0.4$. It can be observed from these figures that the proposed method solution is in excellent agreement with the exact solution.

Table 5.5: L_∞ norm errors for example 5.2.1 when $N = 5000$

α	M	L_∞ errors	order(d)	CPU time(s)
	4	0.0019		7.713
0.3	8	$1.1904e-04$	3.9965	17.671
	16	$8.1775e-06$	3.8636	37.73
	32	$5.3652e-07$	3.9864	124.675
	4	0.0019		30.960
0.4	8	$1.1904e-04$	4.0024	71.697
	16	$7.3759e-06$	4.065	154.018
	32	$4.5491e-07$	4.0012	322.027

Figure 5.4: 3D graph of approximate solution of example 5.2.1 with $M = N = 50$

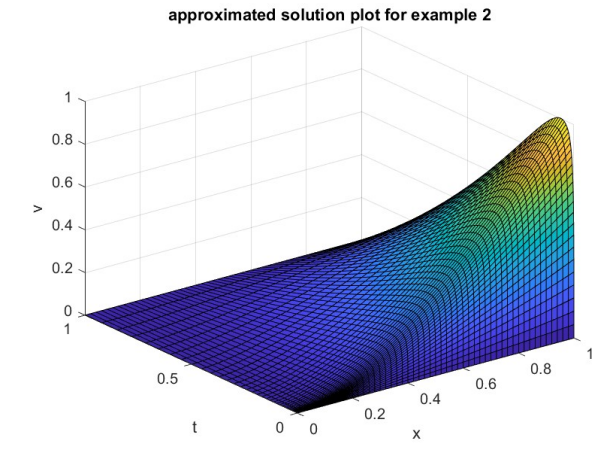

Figure 5.5: 3D graph of exact solution of example 5.2.1 with $M = N = 50$

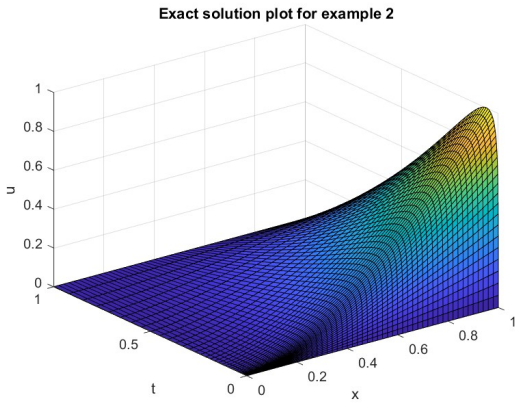

Figure 5.6: 3D graph of error of example 5.2.1

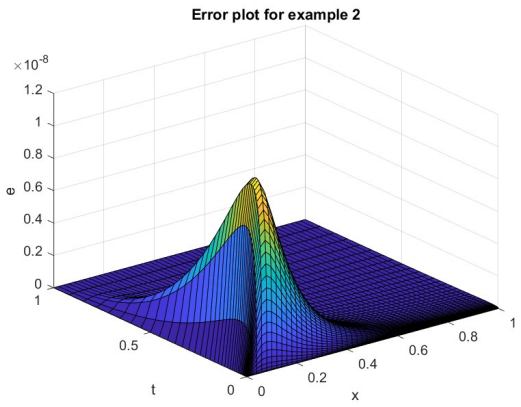

Chapter 6

Conclusion

This research focused on the development of a numerical scheme for the approximation of two distinct time-fractional models under Dirichlet boundary conditions: the nonlinear time-fractional Burgers' Equation and time-fractional Fokker-Planck with variable coefficients.

The fractional derivative in this work was defined using the Caputo formulation, and its temporal discretization was achieved through the L1 scheme implemented on a non-uniform mesh. Numerical examples are presented to showcase the accuracy of the proposed numerical scheme and to validate the derived theoretical error bounds.

Key findings regarding convergence rates include:

- For the TFBE, the graded mesh approach exhibits a convergence order of (2-α) in the temporal direction and second order convergence in the spatial direction. In contrast, the uniform mesh method for the TFBE demonstrates a convergence order of α in the temporal direction.
- A high-order computational scheme was employed for solving the TFFP equation.
- Numerical illustrations are provided to demonstrate the accuracy of the developed numerical scheme and confirm the theoretical error estimates.
- This high-order method for the TFFP achieves a convergence order of (2-α) in the temporal direction and fourth-order convergence in the spatial direction.

Bibliography

[1] D. Baleanu A.Majeed M. Kamran, M.K. Iqbal. Solving time fractional burgers' and fisher's equations using cubic b-spline approximation method. *Springer Nature Link*, 2020(175):–, 2020.

[2] P Roul T Kumari, V Rohil. A computational technique for solving the time-fractional fokker-planck equation. *Mathematical Methods in the Applied Sciences*, 45:9736–9752, 2022.

[3] C. Huang H. Chen, Na An. β-robust superconvergent analysis of a finite element method for the distributed order time-fractional diffusion equation. *Springer Nature Link*, 90(44):39, 2022.

[4] Z. Wang S. Vong. A high order compact finite difference scheme for time fractional fokker–planck equations. *Elsevier Ltd.*, 43(10):39, 2015.

[5] Changqing Fang, Xiaoyin Shen, Kuai He, Chao Yin, Shasha Li, Xinya Chen, and Hongqiang Sun. Application of fractional calculus methods to viscoelastic behaviours of solid propellants. *Philosophical Transactions of the Royal Society A: Mathematical, Physical and Engineering Sciences*, 378:20190291, 2020.

[6] Fayza Alwehebi, Aatef Hobiny, and Dalal Maturi. Variational iteration method for solving time fractional burgers equation using maple. *Applied Mathematics*, 14(5):336–348, 2023.

[7] Swapnali Doley, A. Vanav Kumar, and L. Jino. Numerical study of the time fractional burgers' equation by using explicit and implicit schemes. *Applications and Applied Mathematics: An International Journal (AAM)*, 17:97–107, 2022.

[8] Raghad A. Aljedhi and Adem Kilicman. Derivation of the fractional fokker–planck equation for stable lévy with financial applications. *Mathematics*, 11:1102, 2023.

[9] Mridula Garg and Pratibha Manohar. Analytical solution of space-time fractional fokker planck equations by generalized differential transform method. *Le Matematiche*, 2, 12 2011.

[10] S. G. Rubin and R. A. Graves. A cubic spline approximation for problems in fluid mechanics. Tr r-436, NASA, Washington, DC, 1975.